CHAPTER 5

Theoretical Models and Simulations of Polymer Chains

Andrzej Kloczkowski* and Andrzej Kolinski†

*L .H. Baker Center for Bioinformatics and Biological Statistics, Iowa State University, Ames, IA 50011, USA**; *Faculty of Chemistry, Warsaw University, Pasteura 1, 02-093 Warsaw, Poland*†

5.1 INTRODUCTION

In the first part of this article the review of various theoretical models for polymer chains is given. The models of freely jointed chains, freely rotating chains (including wormlike chains), and chains with fixed bond angles and independent rotational potentials and with interdependent potentials, including rotational isomeric state approximation, are presented.

In the second part various theories of polymer networks are presented. The affine network model, phantom network, and theories of real networks are discussed. Scattering from polymer chains is also briefly presented.

The third part of this article covers computer simulations of polymer chains. Methods of simulation of chains on lattices are presented and the equivalence between lattice chains and off-lattice chain models is discussed. The simulation of excluded volume effect is examined. The polymer chain collapse from random coil to dense globular state, and simulations of dense polymer systems are discussed.

This article describes models for linear chains of homopolymers and for unimodal, unfilled polymer networks. Theoretical models for other systems, such as star, branched, and ring polymers, random and alternating copolymers, graft and block copolymers are discussed in the book by Mattice and Suter [1]. Block copolymers are discussed in Chap. 32 of this Handbook [2]. Theories of branched and ring polymers are presented in the book by Yamakawa [3]. Liquid–crystalline polymers are discussed in the book by Grosberg and Khokhlov [4], and liquid crystalline elastomers in the recent book of Warner and Terentjev [5]. Bimodal networks are discussed by Mark and Erman [6,7]. Molecular theories of filled polymer networks are presented by Kloczkowski, Sharaf and Mark [8] and recently by Sharaf and Mark [9].

This first part of this article deals only with treatment of ''bonded'' interactions of polymer chains, appropriate only for modeling chains under Θ-point conditions. Problems connected with effects of excluded volume are presented at the end of this chapter. The excluded volume effect for chains in good solvents are also presented in Chaps. IIB [10] and IIID [11] of this handbook and in books by Freed [12], de Gennes [13], des Cloizeaux and Jannink [14], and

Forsman [15]. More information about computer modeling of polymers is provided by Binder [16,17], Baumgartner [18], Kolinski and Skolnick [19], and most recently by Kotelyanskii and Therodorou [20].

5.2 THE FREELY JOINTED CHAIN

The freely jointed chain model (known also as random flight model) was proposed for polymers by Kuhn in 1936. The chain is assumed to consist of n bonds of equal length l, jointed in linear succession, where the directions (θ, ϕ) of bond vectors may assume all values $(0 \le \theta \le \pi; 0 \le \phi \le 2\pi)$ with equal probability (see Fig. 5.1).

This means that directions of neighboring bonds are completely uncorrelated. The freely jointed chain model corresponds to a chain with fixed bond lengths and with unconstrained, free to adjust valence angles and with free torsional rotations. The mean square end-to-end vector $\langle r^2\rangle_0$ in the unperturbed state (denoted by subscript 0) for the freely jointed chain is

$$\langle r^2\rangle_0 = \langle (\sum_{i=1}^{n} \mathbf{l}_j)\cdot(\sum_{j=1}^{n}\mathbf{l}_j)\rangle_0 = nl^2 \tag{5.1}$$

because

$$\langle \mathbf{l}_i \cdot \mathbf{l}_j\rangle_0 = 0 \quad \text{for } i \neq j. \tag{5.2}$$

It is convenient to compare real polymer chains with freely jointed chain by using the concept of the characteristic ratio defined as the ratio of the mean-square end-to-end vectors of a real chain and freely jointed chain with the same number of bonds

$$C_n = \frac{\langle r^2\rangle_0}{nl^2}. \tag{5.3}$$

The characteristic ratio is a measure of chain flexibility. Flexible chains have C_n close to unity, while semiflexible and rigid polymers have usually much larger values of C_n. The mean-square radius of gyration for freely jointed chain is:

$$\langle s^2\rangle_0 \equiv \frac{\sum\limits_{0 \le i < j \le n} \langle r_{ij}^2\rangle_0}{(n+1)^2} = \frac{(n+2)nl^2}{6\ (n+1).} \tag{5.4}$$

For longer chains (in the limit $n \to \infty$) we have

$$\frac{\langle s^2\rangle_0}{\langle r^2\rangle_0} = \frac{1}{6}. \tag{5.5}$$

The freely jointed chain model has an exact analytical solution for the distribution function of the end-to-end vector. The probability that the chain of n bonds has the end-to-end vector $\mathbf{r}$ is

$$P(\mathbf{r},n) = \int \mathrm{d}\mathbf{l}_1\mathrm{d}\mathbf{l}_2\ldots\mathrm{d}\mathbf{l}_n\delta[(\sum_{i=1}^{n}\mathbf{l}_i) - \mathbf{r}]\prod_{j=1}^{n}\exp\left(\frac{-\mathrm{u}(\mathbf{l}_j)}{kT}\right), \tag{5.6}$$

where T is the absolute temperature, k is the Boltzmann constant, $u(\mathbf{l}_j)$ is the potential energy of two segments connected by the j-th bond $\mathbf{l}_j$, and δ denotes Dirac delta function. For the freely jointed chain model we have

$$\exp\left(\frac{-\mathrm{u}(\mathbf{l}_j)}{kT}\right) = \frac{1}{4\pi l^2}\delta(|\mathbf{l}_j| - \ell). \tag{5.7}$$

By using the Fourier representation of the δ function we obtain

$$\begin{aligned} P(\mathbf{r},\ n) &= \frac{1}{8\pi^3}\int \mathrm{d}\mathbf{k}\,\mathrm{e}^{-\mathrm{i}\mathbf{k}\cdot\mathbf{r}}\left[\frac{\sin(kl)}{kl}\right]^n \\ &= \frac{1}{2\pi^2 r}\int_0^\infty \sin(kr)\left[\frac{\sin(kl)}{kl}\right]^n k\mathrm{d}k. \end{aligned} \tag{5.8}$$

The solution of Eq. (5.8) is

$$P(\mathbf{r},\ n) = \frac{1}{2^{n+1}\pi l^2 r(n-2)!}\sum_{i=0}^{i\le(n-r/l)/2} (-1)^i\frac{n!}{i!(n-i)!}(n-2i-r/l)^{n-2}. \tag{5.9}$$

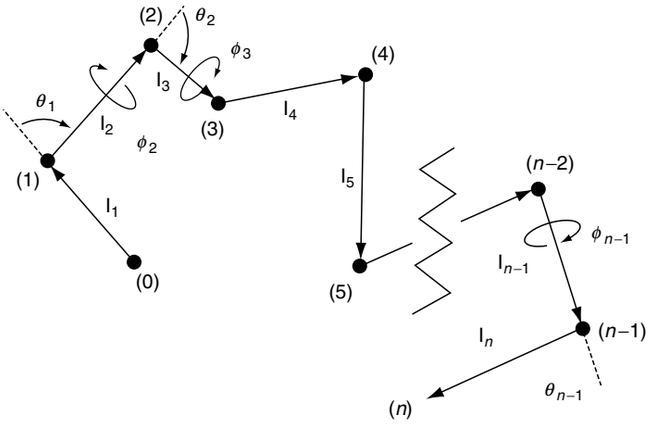

FIGURE 5.1. Polymer chain composed of n bonds. Angles θ are defined as complementary angles.

In the limit $n \to \infty$ the distribution function of the end-to-end vector for freely jointed chain asymptotically approaches a Gaussian function

$$P(\mathbf{r}, n) = \left(\frac{3}{2\pi n l^2}\right)^{3/2} \exp\left(\frac{-3r^2}{2nl^2}\right). \tag{5.10}$$

5.3 THE FREELY ROTATING CHAIN

The freely rotating chain model is a freely-jointed chain with fixed bond angles. It is assumed that all bond have equal length l and all bond angles are equal. The angle θ_i is defined as a supplementary angle of the skeletal bond angle at segment i as seen in Fig. 5.1, and therefore

$$\langle \mathbf{l}_{i+1} \cdot \mathbf{l}_j \rangle = l^2 \cos\theta. \tag{5.11}$$

Similarly for two bonds i and $i+k$ we have

$$\langle \mathbf{l}_{i+k} \cdot \mathbf{l}_i \rangle = l^2 (\cos\theta)^k. \tag{5.12}$$

This result follows from the fact that the projection of a given bond on the preceding bond is $\cos\theta$, while projections in two transverse directions averaged over free rotations are zero. This means that the projection of the $k+i$ bond on the $k+i-1$ bond is $\cos\theta$, the projection of this projection on the $k+i-2$ bond is $(\cos\theta)^2$, etc., which finally leads to the Eq. (5.12). The mean square end-to-end vector for freely rotating chain is

$$\begin{aligned}\langle r^2 \rangle &= \sum_{i=1}^{n} \langle \mathbf{l}_i \rangle^2 + 2 \sum_{i=1}^{n} \sum_{k=1}^{n-i} \langle \mathbf{l}_i \cdot \mathbf{l}_{j+k} \rangle \\ &= nl^2 \left[\frac{1+\cos\theta}{1-\cos\theta} - \frac{2\cos\theta[1-(\cos\theta)^n]}{n(1-\cos\theta)^2} \right]. \end{aligned} \tag{5.13}$$

For infinitely long chains the second term in Eq. (5.13) may be neglected and the characteristic ratio defined by Eq. (5.3) becomes:

$$C_\infty = \frac{1+\cos\theta}{1-\cos\theta}. \tag{5.14}$$

The mean square radius of gyration (defined by Eq. (5.4)) for freely rotating chain is

$$\begin{aligned}\frac{\langle s^2 \rangle_0}{nl^2} &= \frac{(n+2)(1+\cos\theta)}{6(n+1)(1-\cos\theta)} - \frac{\cos\theta}{(n+1)(1-\cos\theta)^2} \\ &\quad + \frac{2(\cos\theta)^2}{(n+1)^2(1-\cos\theta)^3} \\ &\quad - \frac{2(\cos\theta)^3[1-(\cos\theta)^n]}{n(n+1)^2(1-\cos\theta)^4}. \end{aligned} \tag{5.15}$$

For very long chains the last three terms in Eq. (5.15) become negligible and $\langle s^2 \rangle_0 = \langle r^2 \rangle_0 / 6$.

5.3.1 Worm-like Chain Model

The projection of the end-to-end vector of a chain $\mathbf{r}$ on the direction of the first bond $\mathbf{l}_1/l$ for the freely rotating chain is

$$\begin{aligned}\left\langle \frac{\mathbf{r} \cdot \mathbf{l}_1}{l} \right\rangle &= \frac{1}{l} \sum_{i=1}^{n} \langle \mathbf{l}_1 \cdot \mathbf{l}_i \rangle = l \sum_{i=0}^{n-1} (\cos\theta)^i \\ &= l \frac{1-(\cos\theta)^n}{1-\cos\theta}, \end{aligned} \tag{5.16}$$

where θ is the angle between bonds. In the limit $n \to \infty$ this converges to

$$\lim_{n\to\infty} \left\langle \frac{\mathbf{r} \cdot \mathbf{l}}{l} \right\rangle = \frac{1}{1-\cos\theta} \equiv a. \tag{5.17}$$

The quantity a is called the persistence length and is a measure of chain stiffness. The wormlike chain model (sometimes called the Porod-Kratky chain) is a special continuous curvature limit of the freely rotating chain, such that the bond length l goes to zero and the number of bonds n goes to infinity, but the contour length of the chain $L = nl$ and the persistance length a are kept constant. In this limit

$$\left\langle \frac{\mathbf{r} \cdot \mathbf{l}_1}{l} \right\rangle = a(1 - e^{-L/a}) \tag{5.18}$$

and

$$\frac{\langle r^2 \rangle_0}{L} = 2a\left[1 - \frac{a}{L}(1 - e^{-L/a})\right]. \tag{5.19}$$

When the chain length L is much larger than the persistance length a, the effect of chain stiffness becomes negligible. In the limit $L \to \infty$ we have $\langle r^2 \rangle_0 / L \to 2a$ and the wormlike chain reduces to a freely-jointed chain.

5.4 CHAINS WITH FIXED BOND ANGLES AND INDEPENDENT POTENTIALS FOR INTERNAL BOND ROTATION

The more realistic model than freely rotating chain is a chain with fixed bond angles and hindered internal rotations. For simplicity it is assumed that the total configurational energy of the chain is a sum of configurational energies of chain bonds, and the energy of a given bond is independent on the configurational states of other bonds in the chain including the neighboring bonds. We should note that this is an approximation and for real polymer chains because of the steric interactions the energy of a given bond depends on the energy of its neighbors.

We define a local Cartesian coordinate system for each of the bonds. We assume that the axis x_i is directed along the bond i, and the y_i axis lies in the plane formed by bonds i and $i-1$, while the z_i axis is directed to make the coordinate system right-handed. The components of the $(i+1)$th bond $\mathbf{l}_{i+1}$ can be expressed in the coordinate system of the preceding bond i

$$\mathbf{l}'_{i+1} = \mathbf{T}_i \mathbf{l}_{i+1}, \tag{5.20}$$

where $\mathbf{T}_i$ is the orthogonal matrix of the rotational transformation

$$\mathbf{T}_i = \begin{bmatrix} \cos\theta_i & \sin\theta_i & 0 \\ \sin\theta_i\cos\phi_i & -\cos\theta_i\cos\phi_i & \sin\phi_i \\ \sin\theta_i\sin\phi_i & -\cos\theta_i\sin\phi_i & -\cos\phi_i \end{bmatrix} \quad (5.21)$$

Here θ_i is the supplementary bond angle (see Fig. 5.1) and ϕ_i is a dihedral angle between two planes defined by two pairs of bonds: bonds $i-1$ and i, and i and $i+1$.

The scalar product of two bonds $\mathbf{l}_i \cdot \mathbf{l}_j$ written in the matrix notation is $\mathbf{l}_i^{\mathrm{T}}\mathbf{l}_j$ where $\mathbf{l}_j$ is the column vector and $\mathbf{l}_i^{\mathrm{T}}$ is the transpose of $\mathbf{l}_i$ (i.e., the row vector)

$$\mathbf{l}_j = l_j \begin{bmatrix} 1 \\ 0 \\ 0 \end{bmatrix} \quad \mathbf{l}_i^{\mathrm{T}} = \mathbf{l}_j[100], \quad (5.22)$$

where l_i and l_j are lenghts of bonds i and j ($l_i = l_j = l$ in our model but for polymers with different types of bonds in the backbone they may differ). Transforming successively over the intervening bonds the vector representation of the bond j to the coordinate system of bond i ($j > i$) we have

$$\langle \mathbf{l}_i \cdot \mathbf{l}_j \rangle = \langle \mathbf{l}_i^{\mathrm{T}} \mathbf{T}_i \mathbf{T}_{i+1} \cdots \mathbf{T}_{j-1} \mathbf{l}_j \rangle = l_i l_j \langle \mathbf{T}_i \mathbf{T}_{i+1} \cdots \mathbf{T}_j \rangle_{11}. \quad (5.23)$$

Here $\langle \mathbf{T}_i \mathbf{T}_{i+1} \ldots \mathbf{T}_{j-1} \rangle_{11}$ denotes configurational average of the (1–1) element of the matrix product $\mathbf{T}_i \mathbf{T}_{i+1} \ldots \mathbf{T}_{j-1}$. The configurational average of the product of rotational transformation matrices is generally given by

$$\langle \mathbf{T}_i \mathbf{T}_{i+1} \cdots \mathbf{T}_{j-1} \rangle = \frac{\int \cdots \int (\mathbf{T}_i \mathbf{T}_{i+1} \cdots \mathbf{T}_{j-1}) \exp\left[\frac{-E(\mathbf{l}_1, \mathbf{l}_2, \cdots, \mathbf{l}_n)}{kT}\right] \mathrm{d}\mathbf{l}_1 \mathrm{d}\mathbf{l}_2 \cdots \mathrm{d}\mathbf{l}_n}{\int \cdots \int \exp\left[\frac{-E(\mathbf{l}_1, \mathbf{l}_2, \cdots, \mathbf{l}_n)}{kT}\right] \mathrm{d}\mathbf{l}_1 \mathrm{d}\mathbf{l}_2 \cdots \mathrm{d}\mathbf{l}_n}, \quad (5.24)$$

where k is the Boltzmann constant, T is the absolute temperature and $E(\mathbf{l}_1, \mathbf{l}_2, \ldots, \mathbf{l}_n)$ is the conformational energy of the whole chain of n bonds. For a chain with fixed bond lenghts this energy depends only on the orientations of bonds described by bond angles θ_i and rotational angles ϕ_i, where $1 \le i \le n-1$, since the orientation of the last n-th bond is fully determined by the orientation of preceding bonds. For a chain with fixed bond angles the conformational energy is only a function of rotational angles ϕ_i, with $2 \le i \le n-1$, because ϕ_1 is undefined. For chains with independent potentials for internal bond rotation the conformational energy of the chain is a sum of bond energies $E_i(\phi_i)$

$$E(\phi_2, \phi_3, \cdots, \phi_{n-1}) = \sum_{i=2}^{n-1} E_i(\phi_i) \quad (5.25)$$

and

$$\langle \mathbf{T}_i \mathbf{T}_{i+1} \cdots \mathbf{T}_{j-1} \rangle = \prod_{k=1}^{j-1} \langle \mathbf{T}_k \rangle, \quad (5.26)$$

where for symmetric rotational potentials with $u_i(\phi_i) = u_i(-\phi_i)$ we have

$$\langle \mathbf{T}_k \rangle = \begin{bmatrix} \cos\theta_k & \sin\theta_k & 0 \\ \sin\theta_k\langle\cos\phi_k\rangle & -\cos\theta_k\langle\cos\phi_k\rangle & 0 \\ 0 & 0 & -\langle\cos\phi_k\rangle \end{bmatrix}. \quad (5.27)$$

Here $\langle \cos\phi_k \rangle$ is

$$\langle \cos\phi_k \rangle = \frac{\int_0^{2\pi} \cos\phi_k \exp\left[\frac{-E_k(\phi_k)}{kT}\right] \mathrm{d}\phi_k}{\int_0^{2\pi} \exp\left[\frac{-E_k(\phi_k)}{kT}\right] \mathrm{d}\phi_k}. \quad (5.28)$$

Using Eqs. (5.23) and (5.27) we may calculate the mean-square end-to-end vector for fixed bond angles and independent potentials for internal bond rotation

$$\langle r^2 \rangle_0 = nl^2 + 2l^2 \left[\sum_{i=1}^{n} \sum_{k=1}^{n-i} \langle \mathbf{T} \rangle^k \right]_{11} = nl^2 \left[\frac{\mathbf{E} + \langle \mathbf{T} \rangle}{\mathbf{E} - \langle \mathbf{T} \rangle} - 2\langle \mathbf{T} \rangle \frac{(\mathbf{E} + \langle \mathbf{T} \rangle^n)}{n(\mathbf{E} - \langle \mathbf{T} \rangle)^2} \right]_{11}, \quad (5.29)$$

where $\mathbf{E}$ is the unit matrix, and the subscript 11 denotes the (1–1) element of the matrix in square parenthesis. Equation (5.29) resembles Eq. (5.13) for freely rotating chain with $\cos\theta$ replaced by $<\mathbf{T}>$. Similarly to Eq. (5.15) the mean square radius of gyration is

$$\frac{\langle s^2 \rangle_0}{nl^2} = \left[\frac{(n+2)(\mathbf{E} + \langle \mathbf{T} \rangle)}{6(n+1)(\mathbf{E} - \langle \mathbf{T} \rangle)} - \frac{\langle \mathbf{T} \rangle}{(n+1)(\mathbf{E} - \langle \mathbf{T} \rangle)^2} + \frac{2\langle \mathbf{T} \rangle^2}{(n+1)^2(1 - \langle \mathbf{T} \rangle)^3} - \frac{2\langle \mathbf{T} \rangle^3 [1 - \langle \mathbf{T} \rangle^n]}{n(n+1)^2(1 - \langle \mathbf{T} \rangle)^4} \right]_{11}. \quad (5.30)$$

The general solution of eqs. (5.27) and (5.28) is possible by diagonaliziation of the matrix $<\mathbf{T}>$ defined by Eq. (5.27). The eigenvalues of $<\mathbf{T}>$ are

$$\lambda_{1,2} = \frac{1}{2}\left[\cos\theta(1 - \langle\cos\phi\rangle) \pm \sqrt{\cos^2\theta(1 - \langle\cos\phi\rangle)^2 + 4\langle\cos\phi\rangle} \right]. \quad \lambda_3 = -\langle\cos\phi\rangle \quad (5.31)$$

For example, the expression for $\langle r^2 \rangle_0$ in terms of eigenvalues of $<\mathbf{T}>$ is

$$\frac{\langle r^2 \rangle_0}{nl^2} = \frac{(1 + \cos\theta)(1 + \langle\cos\phi\rangle)}{(1 - \cos\theta)(1 - \langle\cos\phi\rangle)} - \frac{2\lambda_1(\cos\theta\langle\cos\phi\rangle + \lambda_1)(1 - \lambda_1^n)}{n(\lambda_1 - \lambda_2)(1 - \lambda_1)^2} + \frac{2\lambda_2(\cos\theta\langle\cos\phi\rangle + \lambda_2)(1 - \lambda_2^n)}{n(\lambda_1 - \lambda_2)(1 - \lambda_2)^2}. \quad (5.32)$$

For very long chains only first terms in Eqs. (5.29) and (5.30) are important and we have

$$C_\infty = \lim_{n\to\infty} \frac{\langle r^2 \rangle_0}{nl^2} = \left[\frac{\mathbf{E} + \langle \mathbf{T} \rangle}{\mathbf{E} - \langle \mathbf{T} \rangle} \right]_{11} = \frac{(1 + \cos\theta)(1 + \langle\cos\phi\rangle)}{(1 - \cos\theta)(1 - \langle\cos\phi\rangle)} \quad (5.33)$$

and

$$\frac{\langle s^2\rangle_0}{nl^2} = \frac{n+2}{6(n+1)} = \left[\frac{\mathbf{E}+\langle\mathbf{T}\rangle}{\mathbf{E}-\langle\mathbf{T}\rangle}\right]_{11} = \frac{(n+2)(1+\cos\theta)(1+\langle\cos\phi\rangle)}{6(n+1)(1-\cos\theta)(1-\langle\cos\phi\rangle)}. \tag{5.34}$$

5.5 CHAINS WITH INTERDEPENDENT ROTATIONAL POTENTIALS. THE ROTATIONAL ISOMERIC STATE APPROXIMATION

In real polymer chains the rotational potentials depend on the steric interactions between pendant groups of neighboring bonds, and are generally not mutually independent. In the simplest case of hydrocarbons the bond rotational potential has three minima as shown in Fig. 5.2. The global minimum at the torsional angle 0° corresponds to the *trans* two other minima with the same energies at torsional angle around $+120^\circ$ and -120° correspond to the *gauche*$^+$ and the *gauche*$^-$ states (g^+ and g^-). The energy difference between the *trans* the *gauche*$^\pm$ states for *n*-alkanes is about 500 cal/(mole). We may use the rotational isomeric state approximation that each bond in the chain occur in one of these rotational states. This assumption enables us to replace all integrals over rotational angles in the partition function and statistical averages by summations over bonds rotational states. Additionally steric interactions between pendant groups of neighboring bonds become important, e.g., the sequence $g^\pm g^\pm$ becomes energetically very unfavorable.

We may neglect the longer range interactions and assume that the configurational energy is a sum of energies of nearest-neighbor pairs

$$E(\phi_2,\phi_3,\cdots,\phi_{n-1}) = \sum_{i=2}^{n-1} E_i(\phi_{i-1},\phi_i). \tag{5.35}$$

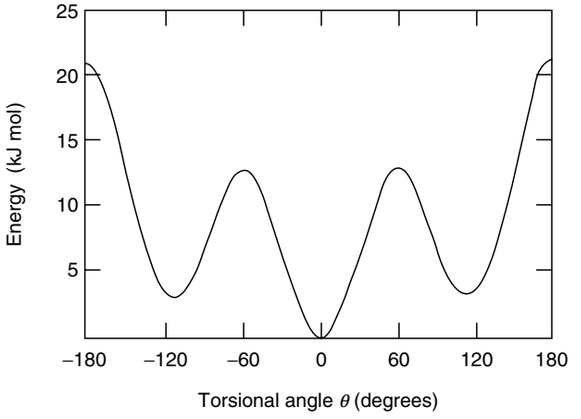

FIGURE. 5.2. The dependence of the conformational energy on the torsional angle in *n*-alkanes.

The configurational partition function becomes

$$Z = \int\cdots\int \exp\left[-\frac{1}{kT}E(\phi_2,\cdots,\phi_{n-1})\right] d\phi_2\cdots d\phi_{n-1} = \sum_{\{\phi\}}\prod_{i=2}^{n-1}\exp\left[-\frac{1}{kT}E_i(\phi_{i-1},\phi_i)\right], \tag{5.36}$$

where $\{\phi\}$ denotes the set of all available states (t,g^+,g^-) for all bonds in the chain. We define the statistical weight corresponding to bond i being in the η state while bond $i-1$ being in the ζ state (where η and ζ are sampled from the t,g^+,g^- set)

$$u_{\zeta\eta,i} = \mathbf{exp}\left(\frac{-E_{\zeta\eta,i}}{kT}\right) \tag{5.37}$$

and the statistical weight matrix

$$\mathbf{U}_i = \begin{bmatrix} u_{tt,i} & u_{tg^+,i} & u_{tg^-,i} \\ u_{g^+t,i} & u_{g^+g^+,i} & u_{g^+g^-,i} \\ u_{g^-t,i} & u_{g^-g^+,i} & u_{g^-g^-,i} \end{bmatrix}. \tag{5.38}$$

It is convenient to express the energy of a given single bond relative to the energy of the *trans* state. The energy of a pair of bonds $E_{\eta\zeta,i}$ is defined relative to the state where the bond i is in the *trans* state, and all subsequent bonds $j > i$ are also in the *trans* states. From this definition follows $E_{\eta t} = 0$ for $\zeta = t,g^+,g^-$. Additionally $E_{tg^+} = E_{tg^-} = E_{g^+g^+} = E_{g^-g^-}$ ($\approx$ 500 cal/mol for *n*-alkanes), and $\mathrm{E_{g^+g^-}} = \mathrm{E_{g^-g^+}}$ ($\approx$ 3,000 cal/mole for *n*-alkanes). This means that the statistical weight matrix may be written as

$$\mathbf{U} = \begin{bmatrix} 1 & \sigma & \sigma \\ 1 & \sigma\psi & \sigma\omega \\ 1 & \sigma\omega & \sigma\psi \end{bmatrix}, \tag{5.39}$$

where $\sigma\psi$ and $\sigma\omega$ denote $u_{g^+g^+}$ and $u_{g^+g^-}$, respectively.

By using the statistical weight matrices we may express the configuration partition function as

$$\mathbf{Z} = \sum_{\{\phi\}}\prod_{i=2}^{n-1} u_{\eta\zeta,i} = \mathbf{J}^*\left[\prod_{i=2}^{n-1}\mathbf{U_i}\right]\mathbf{J}, \tag{5.40}$$

where $\mathbf{J}^*$ and $\mathbf{J}$ are row and column vectors, respectively

$$\mathbf{J}^* = [\,1 \quad 0 \quad 0\,] \quad \mathbf{J} = \begin{bmatrix} 1 \\ 1 \\ 1 \end{bmatrix}. \tag{5.41}$$

For very long chains (in the limit $n \to \infty$) the partition function is determined by the largest eigenvalue λ_1 of the statistical weight matrix $\mathbf{U}$

$$Z \cong \lambda_1^{n-2}. \tag{5.42}$$

The largest eigenvalue of the matrix $\mathbf{U}$ defined by Eq. (5.39) is

$$\lambda_1 = \frac{1}{2}\left[1+\sigma(\psi+\omega)+\sqrt{[1-\sigma(\psi+\omega)]^2+8\sigma}\right]. \tag{5.43}$$

The probability that bonds $i-1$ and i occur in states η and ζ, respectively is

$$p_{\eta\zeta,i} = \frac{1}{Z}\mathbf{J}^*\left[\prod_{k=2}^{i-1}\mathbf{U}_k\right]\frac{\partial \mathbf{U}_i}{\partial \ln u_{\eta\zeta,i}}\left[\prod_{k=i+1}^{n-1}\mathbf{U}_k\right]\mathbf{J} \cong \frac{\partial \ln \lambda_1}{\partial \ln u_{\eta\zeta}}. \tag{5.44}$$

The probability that bond i is in the state ζ, irrespective of the state of bond $i-1$ is

$$p_{\zeta,i} = \sum_{n=t,g^+,g^-} p_{\eta\zeta,i} \cong \sum_{\eta=t,g^+,g^-}\frac{\partial \ln \lambda_1}{\partial \ln u_{\eta\zeta}}. \tag{5.45}$$

The conditional probability that bond i is in ζ state, given that bond $i-1$ is in state η is

$$q_{\eta\zeta,i} = \frac{p_{\eta\zeta,i}}{p_{\eta,i-1}}. \tag{5.46}$$

In order to calculate the mean square end-to-end vector or a radius of gyration we have to calculate averages $\langle \mathbf{T}_i\mathbf{T}_{i+1}\ldots\mathbf{T}_{j-1}\rangle$ (Eq. (5.24)). For bonds with independent rotational potentials this average is a product of averages $\langle \mathbf{T}\rangle$ for single bonds. For chains with interactions between neighboring bonds we define for each bond i the supermatrix $\| \mathbf{T}_i \|$ of the order 9×9

$$\| \mathbf{T}_i \| = \begin{bmatrix} \mathbf{T}(\phi_1) & & \\ & \mathbf{T}(\phi_2) & \\ & & \mathbf{T}(\phi_3) \end{bmatrix}_i, \tag{5.47}$$

where $\mathbf{T}$ is rotation matrix given by Eq. (5.21), and the $\phi_1 = 0^\circ, \phi_2 = 120^\circ, \phi_3 = -120^\circ$, are the torsional angles corresponding to the *trans*, *gauche*$^+$ and *gauche*$^-$ states.

We define also a direct product $\mathbf{U}_i \otimes \mathbf{E}_3$ of the statistical weight matrix $\mathbf{U}_i$ (defined by Eq. (5.38)) and the unit matrix of order three $\mathbf{E}_3$.

$$\mathbf{U}_i \otimes \mathbf{E}_3 = \begin{bmatrix} u_{tt}\mathbf{E}_3 & u_{tg^+}\mathbf{E}_3 & u_{tg^-}\mathbf{E}_3 \\ u_{g^+t}\mathbf{E}_3 & u_{g^+g^+}\mathbf{E}_3 & u_{g^+g^-}\mathbf{E}_3 \\ u_{g^-t}\mathbf{E}_3 & u_{g^-g^+}\mathbf{E}_3 & u_{g^-g}\mathbf{E}_3 \end{bmatrix}. \tag{5.48}$$

The statistical average of the product of rotation matrices may then be written as

$$\langle \mathbf{T}_i\mathbf{T}_{i+1}\ldots\mathbf{T}_{j-1}\rangle = \langle \mathbf{T}_i^{(j-i)}\rangle = \frac{1}{Z}\left[(\mathbf{J}^*\mathbf{U}_2^{(i-2)})\otimes\mathbf{E}_3\right]\times [(\mathbf{U}\otimes\mathbf{E}_3)\parallel \mathbf{T} \parallel]_i^{(j-i)}\left[(\mathbf{U}_j^{(n-j)}\mathbf{J})\otimes\mathbf{E}_3\right] \tag{5.49}$$

Then the mean-square end-to-end vector and the mean square radius of gyration are

$$\langle r^2\rangle_0 = nl^2 + 2\sum_{i=1}^{n-1}\sum_{j=i+1}^{n}\mathbf{l}_i^T\langle \mathbf{T}_i^{(j-i)}\rangle\mathbf{l}_j \tag{5.50}$$

and

$$\langle s^2\rangle_0 = \frac{1}{(n+1)^2}\sum_{0\le h\le k\le n}\sum_{i=h+1}^{k}\sum_{j=h+1}^{k}\mathbf{l}_i^T\langle \mathbf{T}^{(j-i)}\rangle\mathbf{l}_j \tag{5.51}$$

with $\langle \mathbf{T}_i^{(j-i)}\rangle$ given by Eq. (5.49). Both $\langle r^2\rangle_0$ and $\langle s^2\rangle_0$ may be written in a more compact form in terms of proper supermatrices. The details are given in Flory's monograph [21]. Additional information is given in the Handbook chapter by Honeycutt [22].

5.6 THEORIES OF POLYMER NETWORKS

5.6.1 The Affine Network

The theory of affine networks was developed by Kuhn and improved by Treloar, and is based on the assumption that the network consists of ν freely-jointed Gaussian chains and the mean-square end-to-end vector of network chains in the undeformed network is the same as of chains in the uncross-linked state. This assumption is supported by experimental data. It is also assumed that there is no change in volume on deformation and the junctions displace affinily with macroscopic deformation. The intermolecular interactions in the model are neglected, i.e., the system is similar to the ideal gas.

The elastic free energy of a chain is related to the distribution function of the end-to-end vector $P(\mathbf{r})$

$$A_{\text{el}} = c(T) - kT\ln P(\mathbf{r}) = A^*(T) + \frac{3}{2}kT\frac{\langle r^2\rangle}{\langle r^2\rangle_0} \tag{5.52}$$

for the Gaussian distribution given by Eq. (5.10). Here $c(T)$ and $A^*(T)$ are constants dependent only on the temperature T, k is a Boltzmann constant, and $\langle r^2\rangle_0$ is the average of the mean-square end-to-end vector in the undeformed state.

The elastic free energy of the network ΔA_{el} relative to the undeformed state is a sum of free energies of individual chains

$$\Delta A_{\text{el}} = \frac{3kT}{2\langle r^2\rangle_0}\sum_{\nu}(r^2 - \langle r^2\rangle_0) = \frac{3}{2}\nu kT\left(\frac{\langle r^2\rangle}{\langle r^2\rangle_0} - 1\right) \tag{5.53}$$

Here $\langle r^2\rangle$ is the end-to-end vector in the deformed state averaged over the ensemble of chains

$$\langle r^2\rangle = \langle x^2\rangle + \langle y^2\rangle + \langle z^2\rangle. \tag{5.54}$$

In the affine model of the network it is assumed all junction points are imbedded in the network, and each Cartesian component of the chain end-to-end vector transforms linearly with macroscopic deformation

$$x = \lambda_x x_0, \quad y = \lambda_y y_0, \quad z = \lambda_z z_0 \tag{5.55}$$

$$\langle x^2\rangle = \lambda_x^2\langle r^2\rangle_0, \quad \langle y^2\rangle = \lambda_y^2\langle y^2\rangle_0, \quad \langle z^2\rangle = \lambda_z^2\langle z^2\rangle_0 \tag{5.56}$$

and therefore

$$\Delta A_{\text{el}} = \frac{1}{2}\nu kT(\lambda_x^2 + \lambda_y^2 + \lambda_z^2 - 3). \tag{5.57}$$

Here, λ_x, λ_y, and λ_z are the components of the deformation tensor $\boldsymbol{\lambda}$, defined as the ratios of the final length of the

sample L_t to the initial length $L_{t,0}$ in $t = x$, y, and z direction, respectively. (The more rigorous statistical mechanical analysis by Flory [23] has shown that Eq. (5.57) should contain additional logarithmic term $-\mu kT \ln(V/V_0)$, where μ is the number of junctions, V is the volume of the network, and V_0 is volume of the network at the state of formation).

The force f under uniaxial tension in direction z is obtained from the thermodynamic expression:

$$f = \left(\frac{\partial \Delta A_{\mathrm{el}}}{\partial L}\right)_{T,V} = L_0^{-1}\left(\frac{\partial \Delta A_{\mathrm{el}}}{\partial \lambda}\right)_{T,V}, \tag{5.58}$$

where $\lambda = \lambda_z = L_z/L_{z,0}$. Because the volume of the sample is constant during deformation the x and y components of the deformation are $\lambda_x = \lambda_y = \lambda^{-1/2}$. Performing the differentiation in Eq. (5.58) leads to the elastic equation of state

$$f = \left(\frac{\nu kT}{L_0}\right)(\lambda - 1/\lambda^2). \tag{5.59}$$

5.6.2 The Phantom Network Theory

The theory of phantom network was formulated by James and Guth [24] in the forties. They assumed that chains are Gaussian with the distribution $P(\mathbf{r})$ of the end-to-end vector

$$P(\mathbf{r}) = \left(\frac{\gamma}{\pi}\right)^{3/2} \exp(-\gamma r^2), \tag{5.60}$$

where

$$\gamma = \frac{3}{2\langle r^2\rangle_0} \tag{5.61}$$

and interact only at junction points. This means that chains may pass freely through one another, i.e., are ''phantom'', the excluded volume effects and chain entanglements are neglected in the theory. They assumed also that all junctions at the surface of the network are fixed and deform affinely with macroscopic strain, while all junctions and chains inside the bulk of the network fluctuate around their mean positions. The idea of the phantom network is very similar to the concept of the ideal gas. The theory based on these simple assumptions leads to significant improvements in the understanding of the properties of networks, such as microscopic fluctuations and neutron scattering behavior.

The configurational partition function Z_N of the phantom network is the product of the configurational partition functions of its individual chains. junctions i and j:

$$Z_N = C\prod_{i<j} \exp(-3r_{ij}^2/2\langle r_{ij}^2\rangle_0) = C\prod_{i<j} \exp\left(-\frac{1}{2}\sum_i \sum_j \gamma_{ij}^* |\mathbf{R}_i - \mathbf{R}_j|^2\right). \tag{5.62}$$

Here, $\mathbf{R}_i$ and $\mathbf{R}_j$ are positions of junctions i and j, $\gamma_{\mathrm{ij}}^* = 3/2\langle r_{\mathrm{ij}}^2\rangle_0$ if junctions i and j are connected by a chain, and zero otherwise, and C is a normalization constant. The position vectors $\mathbf{R}_i$ with i ranging from 1 to μ, where μ is a number of junctions, may be arranged in column form, represented as $\{\mathbf{R}\}$. Equation (5.62) may then be written

$$Z_N = C\exp(-\{\mathbf{R}\}^T \boldsymbol{\Gamma} \{\mathbf{R}\}), \tag{5.63}$$

where the superscript T denotes the transpose. The symmetric matrix $\boldsymbol{\Gamma}$ known as the Kirchhoff valency-adjacency matrix in the graph theory describes the connectivity of the network and its elements γ_{ij} are

$$\boldsymbol{\Gamma} = \begin{cases} \gamma_{ij} = -\gamma_{ij}^*, & i \neq j \\ \gamma_{ii} = \sum_j \gamma_{ij}^* = \sum_j \gamma_{ij}^*. \end{cases} \tag{5.64}$$

James and Guth assumed that all μ junctions in the network may be divided into two sets of junctions: (i) μ_σ fixed junctions at the bounding surface of the polymer and (ii) μ_τ free junctions fluctuating about their mean positions $\{\bar{\mathbf{R}}_\tau\}$ inside the polymer. The partition function of the network due to fluctuating junctions is

$$Z_N = C\exp(-\{\Delta\mathbf{R}_\tau\}^T \boldsymbol{\Gamma}_\tau \{\Delta\mathbf{R}_\tau\}), \tag{5.65}$$

where $\{\Delta\mathbf{R}_\tau\}$ denotes fluctuations of free junctions

$$\{\Delta\mathbf{R}_\tau\} = \{\mathbf{R}_\tau\} - \{\overline{\mathbf{R}}_\tau\}. \tag{5.66}$$

The product of the fluctuations of two junctions i and j averaged over the network may be obtained from Eq. (5.65) as

$$\langle \Delta\mathbf{R}_i \cdot \Delta\mathbf{R}_j\rangle = \frac{\int \Delta\mathbf{R}_i \cdot \Delta\mathbf{R}_j \exp[-\{\Delta\mathbf{R}_\tau\}^{\mathrm{T}} \boldsymbol{\Gamma}_\tau \{\Delta\mathbf{R}_\tau\}]\mathrm{d}\{\Delta\mathbf{R}_\tau\}}{\int \exp[-\{\Delta\mathbf{R}_\tau\}^{\mathrm{T}} \boldsymbol{\Gamma}_\tau \{\Delta\mathbf{R}_\tau\}]\mathrm{d}\{\Delta\mathbf{R}_\tau\}} = -\frac{\partial \ln Z_\tau}{\partial \gamma_{ij}}, \tag{5.67}$$

where $\mathrm{d}\{\Delta\mathbf{R}_\tau\} \equiv \mathrm{d}\Delta\mathbf{R}_{1\tau}\mathrm{d}\Delta\mathbf{R}_{2\tau}\ldots\mathrm{d}\Delta\mathbf{R}_{\mu\tau}$ and

$$Z_\tau = \int \exp[-\{\Delta\mathbf{R}_\tau\}^{\mathrm{T}} \boldsymbol{\Gamma}_\tau \{\Delta\mathbf{R}_\tau]\mathrm{d}\{\Delta\mathbf{R}_\tau\} = \left(\frac{\pi^{\mu_\tau}}{\det\boldsymbol{\Gamma}_\tau}\right)^{3/2}. \tag{5.68}$$

This leads to the expression

$$\langle \Delta\mathbf{R}_i \cdot \Delta\mathbf{R}_j\rangle = \frac{3}{2}\frac{\partial}{\partial \gamma_{ij}} \ln|\det\boldsymbol{\Gamma}_\tau| = \frac{3}{2}(\boldsymbol{\Gamma}_\tau^{-1})_{ij}, \tag{5.69}$$

where $(\boldsymbol{\Gamma}_\tau^{-1})_{ij}$ denotes the $(i-j)$-th element of the inverse matrix $\boldsymbol{\Gamma}_\tau^{-1}$. Fluctuations of junctions from their mean positions in a phantom network depend on the network's functionality ϕ and are independent of macroscopic deformation.

For example for the infinitely large network with the symmetrical tree-like topology (such as shown in Fig. 5.3) the mean-square fluctuations of junctions $\langle(\Delta\mathrm{R})^2\rangle$ and

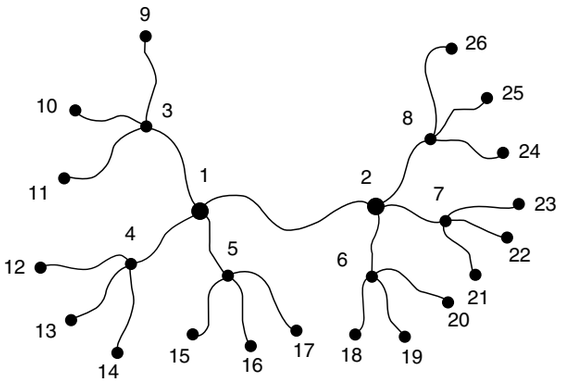

FIGURE 5.3. First three tiers of a unimodal, symmetrically grown, tetrafunctional network ($\phi = 4$) with tree-like topology.

correlations between fluctuations of two junctions i and j $\langle \Delta\mathbf{R}_i \cdot \Delta\mathbf{R}_j \rangle$ separated by m other junctions are:

$$\begin{bmatrix} \langle (\Delta \mathrm{R}_i)^2 \rangle & \langle \Delta\mathbf{R}_i \cdot \mathbf{R}_j \rangle \\ \langle \Delta\mathbf{R}_j \cdot \Delta\mathbf{R}_i \rangle & \langle (\Delta \mathrm{R}_j)^2 \rangle \end{bmatrix} = \frac{3}{2} \begin{bmatrix} (\Gamma_\tau^{-1})_{ii} & (\Gamma_\tau^{-1})_{ij} \\ (\Gamma_\tau^{-1})_{ji} & (\Gamma_\tau^{-1})_{jj} \end{bmatrix}$$

$$= \frac{3}{2\gamma} \begin{bmatrix} \frac{\phi-1}{\phi(\phi-2)} & \frac{1}{\phi(\phi-2)(\phi-1)^m} \\ \frac{1}{\phi(\phi-2)(\phi-1)^m} & \frac{\phi-1}{\phi(\phi-2)} \end{bmatrix}. \tag{5.70}$$

The mean-square fluctuations of the distance $r_{ij} = |\mathbf{R}_i - \mathbf{R}_j|$ between junctions i and j are

$$\begin{aligned} \langle (\Delta r_{ij})^2 \rangle &= \langle (\Delta\mathbf{R}_i - \Delta\mathbf{R}_i)^2 \rangle \\ &= \frac{3}{2}[(\Gamma_\tau^{-1})_{ii} + (\Gamma_\tau^{-1})_{jj} - 2(\Gamma_\tau^{-1})_{ij}] \\ &= \frac{2[(\phi-1)^{m+1} - 1]}{\phi(\phi-2)(\phi-1)^m} \langle r^2 \rangle 0. \end{aligned} \tag{5.71}$$

For a special case of mean-square fluctuations of the end-to-end vector ($m = 0$) we have

$$\langle (\Delta r)^2 \rangle = \frac{2}{\phi} \langle r^2 \rangle_0. \tag{5.72}$$

Equations (5.70) and (5.71) may be easily generalized for fluctuations of points along the chains in the network, since each point along the chain may be considered as bi-functional junction. As a consequence the valence-adjacency matrix in this generalized case contains additional elements describing the connectivity of bi-functional junctions. More details is provided in the review article by Kloczkowski, Mark, and Erman [25].

The vector $\mathbf{r}_{ij}$ between junctions i and j is

$$\boldsymbol{r}_{ij} = \bar{\boldsymbol{r}}_{ij} + \Delta\boldsymbol{r}_{ij}, \tag{5.73}$$

where $\Delta\mathbf{r}_{ij}$ is the instantaneous fluctuation of $\mathbf{r}_{ij}$ and $\bar{\mathbf{r}}_{ij}$ is the time average of $\mathbf{r}_{ij}$. Squaring both sides of the above equation and taking the ensemble average leads to

$$\langle r_{ij}^2 \rangle = \langle \bar{r}_{ij}^2 \rangle + \langle (\Delta r_{ij})^2 \rangle \tag{5.74}$$

since instantaneous fluctuations and mean values are uncorrelated. From Eqs. (5.72) and (5.74) follows:

$$\langle \bar{r}^2 \rangle = (1 - \frac{2}{\phi}) \langle r^2 \rangle_0. \tag{5.75}$$

According to the theory the mean positions of junctions transform affinely with macroscopic strain while the fluctuations are strain independent:

$$\boldsymbol{r}_{ij} = \bar{\boldsymbol{r}}_{ij} + \Delta\boldsymbol{r}_{ij} \tag{5.76}$$

i.e.,

$$\langle r^2 \rangle = \left[(1 - \frac{2}{\phi}) \frac{\lambda_x^2 + \lambda_y^2 + \lambda_z^2}{3} + \frac{2}{\phi} \right] \langle r^2 \rangle_0. \tag{5.77}$$

Using Eq. (5.53) for the elastic free energy, we obtain the following expression for the free energy of the phantom network

$$\Delta A_{\mathrm{el}} = \frac{1}{2}(1 - \frac{2}{\phi}) \nu kT (\lambda_x^2 + \lambda_y^2 + \lambda_z^2 - 3). \tag{5.78}$$

Equation (5.78) is very similar to Eq. (5.57) for the affine network. The only difference is that the so called front factor (equal $\nu/2$ for affine network model) is replaced by $\xi/2$ for the phantom network model where

$$\xi = (1 - \frac{2}{\phi}) \nu. \tag{5.79}$$

The equation for the elastic force is similar to Eq. (5.59) for the affine network with ν replaced by ξ.

5.7 STATISTICAL THEORIES OF REAL NETWORKS

In real polymer network the effects of excluded volume and chain entanglements should be taken into account. In 1977 Flory [26] formulated the constrained junction model of real networks. According to this theory fluctuations of junctions are affected by chains interpenetration, and as the result the elastic free energy is a sum of the elastic free energy of the phantom network ΔA_{ph} (given by Eq. (5.78)) and the free energy of constraints ΔA_{c}

$$\Delta A_{\mathrm{el}} = \Delta A_{\mathrm{ph}} + \Delta A_{\mathrm{c}} \tag{5.80}$$

with ΔA_{c} given by the formula

$$\Delta A_{\mathrm{c}} = \frac{1}{2} \mu kT \sum_{t=x,y,z} [B_t + D_t - \ln(1 + B_t) - \ln(1 + D_t)], \tag{5.81}$$

where

$$B_t = \frac{\kappa^2(\lambda_t^2 - 1)}{(\lambda_t^2 + \kappa^2)^2} \tag{5.82}$$

and

$$D_t = \frac{\lambda_t^2 B_t}{\kappa}. \tag{5.83}$$

Here κ is a parameter which measures the strength of the constraints. For $\kappa = 0$ we obtain the phantom network limit, and for infinitely strong constraints ($\kappa = \infty$) the affine limit is obtained. Erman and Monnerie [27] developed the constrained chain model, where constraints effect fluctuations of the centers of the mass of chains in the network. Kloczkowski, Mark, and Erman [28] proposed a diffused-constraint theory with continuous placement of constraints along the network chains.

A different statistical–mechanical approach based on so called replica formalism was developed by Edwards and coworkers [29,30]. They studied the effect of topological entanglements between chains on the elastic free energy of the network and formulated the slip-link model. The elastic energy of constraints in the slip-link theory is

$$\Delta A_{\mathrm{c}} = \frac{1}{2} N_{\mathrm{s}} kT \sum_{t=x,y,z} \left[\frac{(\lambda_t^2 - 1)}{1 + \eta\lambda_t^2} + \ln \left[\frac{1 + \eta\lambda_t^2}{1 + \eta} \right] \right], \quad (5.84)$$

where N_{s} is the number of slip-links and η is the slipage parameter. Equation (5.84) is very similar to Eq. (5.81) for the constrained junction model. Vilgis and Erman [31] showed that for small deformations both equations have the same form (except minor volume term) with $\kappa = 1/\eta$.

5.8 SCATTERING FROM POLYMER CHAINS

The scattering form factor $S(\mathbf{q})$ from a labeled chain in the network is given by the Fourier transform of the distribution function $\Omega(\mathbf{r}_{ij})$ of the vector $\mathbf{r}_{ij}$ between two scattering centers i and j averaged over all pairs of scattering centers along the chain:

$$S(\mathbf{q}) = \frac{1}{N^2} \sum_{i,j=1}^{N} \int \exp(i\mathbf{q} \cdot \mathbf{r}_{ij}) \Omega(\mathbf{r}_{ij}) \mathrm{d}\mathbf{r}_{ij}. \quad (5.85)$$

Here $\mathbf{q}$ is the scattering vector representing the difference between the incident and scattered wave vectors $\mathbf{k}_0$ and $\mathbf{k}$, respectively, and N is the total number of scattering centers along the chain.

The distribution function $\Omega(\mathbf{r}_{ij})$ of the vector $\mathbf{r}_{ij}$ between scattering centers in the undeformed state is assumed to be Gaussian. The distribution function $\Omega(\mathbf{r}_{ij})$ in the deformed state is

$$\Omega(\mathbf{r}_{ij}) = [(2\pi)^3 \langle x_{ij}^2 \rangle \langle y_{ij}^2 \rangle \langle z_{ij}^2 \rangle]^{-1/2} \exp(- x_{ij}^2/2\langle x_{ij}^2 \rangle - y_{ij}^2/2\langle y_{ij}^2 \rangle - z_{ij}^2/2\langle z_{ij}^2 \rangle), \quad (5.86)$$

where $\langle x_{ij}^2 \rangle$, $\langle y_{ij}^2 \rangle$, and $\langle z_{ij}^2 \rangle$ are the mean-square components of the vector $\mathbf{r}_{ij}$ in the deformed state. Substituting the expression for $\Omega(\mathbf{r}_{ij})$ given by Eq. (5.86) into Eq. (5.85) leads to

$$S(\mathbf{q}) = \frac{1}{N^2} \sum_{i,j=1}^{N} \exp(- q_x^2 \langle x_{ij}^2 \rangle/2 - q_y^2 \langle y_{ij}^2 \rangle/2 - q_z^2 \langle z_{ij}^2 \rangle/2), \quad (5.87)$$

where q_x, q_y, and q_z are the components of the scattering vector $\mathbf{q}$. The vector $\mathbf{r}_{ij}$ between two scattering centers may be written for a phantom network as $\mathbf{r}_{ij} = \bar{\mathbf{r}}_{ij} + \Delta\mathbf{r}_{\mathrm{ij}}$ where $\bar{\mathbf{r}}_{ij}$ is the time average of $\mathbf{r}_{ij}$, and $\Delta\mathbf{r}_{ij}$ is the instantaneous fluctuation of $\mathbf{r}_{ij}$ from its mean time-averaged value. Assuming that mean-square fluctuations are strain independent and that mean positions transform affinely with macroscopic strain and applying Eqs. (5.74)–(5.77) leads to

$$\langle x_{ij}^2 \rangle = \left[\lambda_x^2 + (1 - \lambda_x^2) \frac{\langle \Delta x_{ij}^2 \rangle_0}{\langle x_{ij}^2 \rangle_0} \right] \langle x_{ij}^2 \rangle_0, \quad (5.88)$$

where λ_x is the x component of the principal deformation gradient tensor $\boldsymbol{\lambda}$, with similar expressions for the y and z components. For a freely jointed chain

$$\langle x_{ij}^2 \rangle_0 = \langle r_{ij}^2 \rangle_0 / 3 = \eta \langle r^2 \rangle_0 / 3,$$

where $\eta = |i - j|/N$ is the fractional distance, and $\langle r^2 \rangle_0$ is the mean-square end-to-end vector for the undeformed chain. Substituting these results to Eq. (5.87) leads to

$$S(\mathbf{q}) = \frac{1}{N^2} \sum_{i,j=1}^{N} \exp\left[-\upsilon \frac{|i - j|}{N} \left(1 - (1 - \lambda^{*2}) \frac{(\phi - 2)}{\phi} \frac{|i - j|}{N} \right) \right]. \quad (5.89)$$

In this equation

$$\upsilon = q^2 \langle r^2 \rangle_0 / 6 \quad (5.90)$$

and the *vector* $\boldsymbol{\lambda}^*$ is

$$\boldsymbol{\lambda}^* = \boldsymbol{\lambda}\mathbf{q}/q. \quad (5.91)$$

For scattering parallel to the direction of extension $\lambda^* = \lambda_{\parallel}$ and for scattering perpendicular to the direction of extension $\lambda^* = \lambda_{\perp} = 1/\sqrt{\lambda_{\parallel}}$. Replacing the double summation by integration and evaluating one of the integrals leads to

$$S(\mathbf{q}) = 2 \int_0^1 \mathrm{d}\eta (1 - \eta) \exp\left[-\upsilon\eta \left[1 - \eta(1 - \lambda^{*2}) \frac{\phi - 2}{\phi} \right] \right] \quad (5.92)$$

the result obtained by Pearson [32]. As the strain goes to zero Eq. (5.92) has the limiting form

$$\lim_{\lambda \to 1} S(\mathbf{q}) = \frac{2}{\upsilon} (\mathrm{e}^{-\upsilon} + \upsilon - 1) \quad (5.93)$$

derived by Debye [33], corresponding to the scattering from an unperturbed Gaussian coil. Readers interested in scattering from labeled cross-linked paths in unimodal and bimodal networks should consult the review article by Kloczkowski, Mark, and Erman [25].

5.9 SIMULATIONS OF POLYMERS

System composed of polymers or containing polymers immersed in low molecular media are extremely complex

for many reasons. First, polymer chains (linear, branched, or cyclic) have often a huge molecular mass. Large fraction of single covalent bonds in the main chain imply at least a limited internal rotational freedom for each such bond, and consequently lead to an enormous number of available conformational isomers. Second, due to the excluded volume effect polymer chains are non-Markovian, i.e., conformational space accessible to a selected portion of the chain depends on the actual conformation of the remaining fragments. Consequently, a rigorous analytical treatment of polymer conformational statistics and dynamics is essentially impossible; although various aspects of polymer physics could be quite successfully addressed within framework of approximate theories (see the previous sections). Third, the chain connectivity imposes a complex network of topological obstacles. A moving chain cannot cross its own contour or the paths of the other chains present in the system. This has pronounced consequences for polymer dynamics in solutions and polymeric melts, where motion of polymers has to be extremely correlated and the correlation distances are several orders of magnitude larger than it is observed in typical disordered low molecular systems. The nature of these correlations could be extremely complex.

For the above reasons computer simulations are very important components of methodology of theoretical polymer physics. Properly designed computational experiments expand our understanding of these complex systems, provide excellent test of the existing theories and stimulate development of new theoretical approaches. Due to the large size, time scales involved, and complexity of polymeric systems numerous new simulation techniques have been developed to meet these extreme computational demands. This way theoretical physics of polymers had significant influence on progress in computational physics in general.

Simulations of polymers could be designed on various levels of molecular details treated in an explicit way [16–20, 34–36]. Molecular Dynamics (or Brownian Dynamics) of all-atom systems are limited to short chains or/and to studies of local and fast relaxation processes. It is rather impractical, and often nonfeasible, to do MD simulations of long polymer collapse or a self diffusion of polymer chain in a melt, to give just a couple of typical examples. Monte Carlo simulations of the all-atom systems have a bit less limitations, but still large scale rearrangements are difficult to study. For these reasons frequently reduced representations of polymer conformational space are employed. These range from united atom models, where groups of atoms are treated as single interaction units, to lattice models where entire mers (or large united atoms) are restricted to a lattice, thereby enormously reducing the number of available states and simplifying energy calculations. While simple lattice models are of very limited utility in the physics of low molecular mass system, for polymers they provided general solutions to very fundamental problems. This qualitative difference is strictly related to the difference in the correlation length scales in the two types of systems. In polymers the local details become usually irrelevant at large distances. Because of their importance for general physics of polymers and educational values we start from a discussion of simple lattice models of polymers and polymer dynamics.

5.9.1 Ideal Lattice Chains are Equivalent to Off-lattice Models

Let us consider a chain restricted to a simple cubic lattice, with the lattice spacing equal to 1. The chain is a string of vectors with the six allowed orientations belonging to the following set $\{|1,0,0|, |-1,0,0|, |0,1,0|, |0,-1,0|, 0,0,1, |0,0,-1|\}$. A chain vector could be followed by any of the vectors from the set. Thus, there is no any average orientational correlation between the chain vectors, in spite of the lattice restrictions. Note, that for this ideal model a lattice site can be occupied by more than one bead of the chain. It could be immediately seen that the Eqs. (5.1) and (5.2) written for the freely joined chain are true as well for the ideal lattice chain. The models are equivalent, and an exact analytical theory of their conformational statistics exists. Such analogy goes much further. Let us now consider a chain restricted to the diamond lattice with a constant tetrahedral value of the valence angle and three discrete values of the torsional angle corresponding to the *trans* and two *gauche* states. Again, it is easy to note that this model is equivalent (in respect to its global properties) to the ideal, freely rotating chain with the tetrahedral value of the planar angle. It is also easy to show that such chain can mimic the chain with restricted rotations and interdependent rotations, provided Boltzmann weights are assigned to the *trans* and *gauche* conformations and proper correlations between the weights are taken into account.

Equivalence of the ideal continuous and the lattice models extends also on the dynamic properties of a single chain. The Rouse model [37,38] , (or the bead and spring model) consists of a string of points (or beads) of equal mass connected by harmonic springs of equal length and equal strength of the harmonic potentials, although without any angular interactions. An exact analytical solution for the relaxation spectrum of this model is relatively easy to derive. For the ideal (without excluded volume limitations) lattice chain a simple model of dynamics, simulated by a long random sequence of small local conformational changes, could be formalized in a stochastic Master Equation of motion. It has been shown by Verdier and Stockmayer [39], that such model is equivalent to the Rouse model [37,38] in almost entire relaxation spectrum, except the fastest local oscillations involving a couple of chain segments.

5.9.2 Simulation of the Excluded Volume Effect in a Single Chain

The ideal models described in the previous sections ignored a very important fact, that a polymer has its own volume, i.e., two segments cannot occupy the same place in space. Using a series of approximations Flory has shown that the exclude volume leads to a significant increase of the average random coil dimensions and changes the number of accessible conformers. Flory, has also shown that in a thermodynamically ''poor'' solvent the proper volume of the chain segments could be balanced by their mutual attractions, leading to a pseudoideal state, very similar to the Boyle point for the real gases. Typical, however, is the situation of a ''good'' solvent, where the effect of excluded volume is large. Exact analytical solution to the excluded volume problem does not exist. It is unknown how to calculate partition function of a single chain, since the probability of a given conformation of the $(n+1)$th bond added to a chain depends on the conformation of the preceding n bonds. The process of virtual growth of a ''real'' (with excluded volume, in contrast to the ideal, lacking volume chains) chain is non-Markovian. This is exactly a situation where the data from computer simulations are needed for estimations of true (in silico) experimental properties of the model system and for subsequent evaluation of the assumptions and predictions of various approximate theories.

In the context of a simple lattice model the problem could be formulated as follows. Compute the number of non-self-intersecting random walks on the lattice and the distribution of the segment density, size, shape, etc., of the resulting random coils as a function of the chain length. The first thought is to use computer for an exact enumeration of all possible conformations of a n-segment chain. Unfortunately, the number of possible random walks grows exponentially with the chain length. Exact enumeration is possible only for n range of few tens of segments. In this range the finite length effects are still large and an extrapolation of the obtained (exact) data to higher values of n is uncertain. Another approach is to employ a stochastic sampling (Monte Carlo method) to get a ''representative'' ensemble of non-self-intersecting random walks of the assumed length n. There the result is not exact, however avoids any systematic errors. The magnitude of the statistical error could be always reduced by the increase of the sample size. The algorithm is very simple.

1. Start from the first bond.
2. Add the next bond in a randomly selected direction (the simple ''back'' step could be a priori prohibited and the resulting bias easily removed from the results).
3. Check for non-self-intersection and repeat from (2) if a double occupancy of a lattice site is not detected, otherwise erase the chain and start from (1).
4. Stop the chain growth when the requested length n is reached and add the chain to the statistical ensemble.
5. Repeat the entire process starting from (1) until the required number of chain in the sample is collected.
6. Perform statistical analysis of the collected ensemble.

The process of the MC chain growth is illustrated in Fig. 5.4.

Situations, as that schematically depicted in Fig. 5.4B happen quite frequently. Therefore, the algorithm outlined above has a huge sample attrition rate; only a small fraction of the staring chains are finally accepted in the statistical

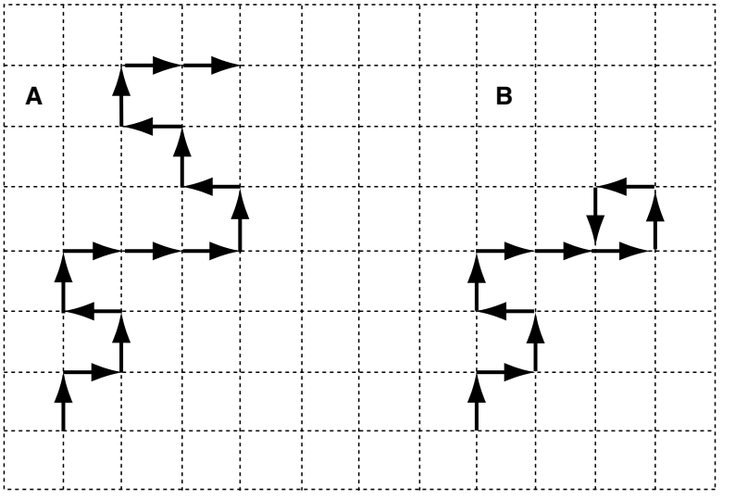

FIGURE 5.4. Two dimensional illustration of the MC growth of non-self-intersecting walks (see the text for details). On the left side (A) an example of the successful structure composed of $n = 15$ segments is shown. On the right side (B) an intersection has been detected before reaching $n = 15$, the final chain length, and the chain has to be removed from the statistical ensemble.

pool. To overcome this problem Rosenbluth and Rosenbluth [40] proposed a modified approach. The segments are selected only from the set of orientations which do not cause the intermediate chain clash. In the case shown in Fig. 5.4B the segment number 11 would be selected only from the following two possibilities; to the left, and to the top of the plane. Obviously, this introduces a bias to the sample. This bias could be easily removed with a proper weighting of the particular conformation with a factorials depending on the number of the allowed continuations at each step. The R&R method allows for generation of much longer chains. Their length is limited by the ''cull-the-sack'' effect, where the growing chain end is surrounded by the chain segments, blocking all the possibilities for the further continuation of the growth process. A number of extensions of the original R&R method have been proposed since then. In general, these methods look into possibility of a continuation in a larger perspective than just one segment ahead.

There are several qualitatively different ways of sampling the polymer conformational space. One may start from a chain of a given length and successively modify its conformation. Two examples of such types of algorithms are illustrated in Fig. 5.5. One of them is the ''pivot'' algorithm, where a single step consist of a random selection of a bond and a rotation (in two dimensional case it is reduced just to a flip; vertical or horizontal) of the selected end of the chain. Advantage of this algorithm is that in a single step a large modification of the chain conformation is attempted. However the acceptance rate for longer chain could be rather small. A number of different global rearrangements of the chain conformations were designed aiming on a more efficient sampling. An example is the ''reptation'' algorithm, where a bond (or a small number of bonds) is cut-off from one end of the chain and added in a random direction on the opposite end. The acceptance ratio for this type of global update algorithms could be quite high. Yet another example is a technique that could be viewed as a complex ''pivot-like'' algorithm, where a part of the chain on one end is erased and then re-grown in a random or semirandom fashion. Of course, the statistical sample is collected in along series of attempts (sometimes successful) to successive modifications of subsequently generated conformations. In the second type of algorithms (Fig. 5.5A) local micromodiffications of the chain conformation are randomly selected at random position of the chain. Marginally, let us note that the local move algorithm could be interpreted as a simulated Brownian motion of a polymer chain. This is a ''real'' chain version of the before mentioned Verdier–Stockmayer model [39] of polymer dynamics. Again, it should be stressed out, that an accurate analytical theory for the real chain dynamics does not exist. The local move algorithms are powerful tools for study of long-time (and large scale) polymer dynamics. There are however several problems with the models employing a limited set of local moves and low coordination number lattices. The algorithms could be nonergodic, or rather ergodic in a subset of its full conformational space. This is explained in Fig. 5.6. There is no path to- and no path from the conformation shown in the drawing. The problem may be cured using a higher coordination lattices and/or a larger set of ''less-local'' micromodiffications. An example of such larger scale move is shown in Fig. 5.6B. The backfire of such update of the local move algorithms is a less clear relation with the model of the Brownian motion. Perhaps, the ''wave-like'' move, when attempted rarely could be interpreted as a particular coincidence of a series of local moves, which somehow were able to pass the local conformational barriers. An additional flaw of the low coordination lattice models (beside the ergodicity

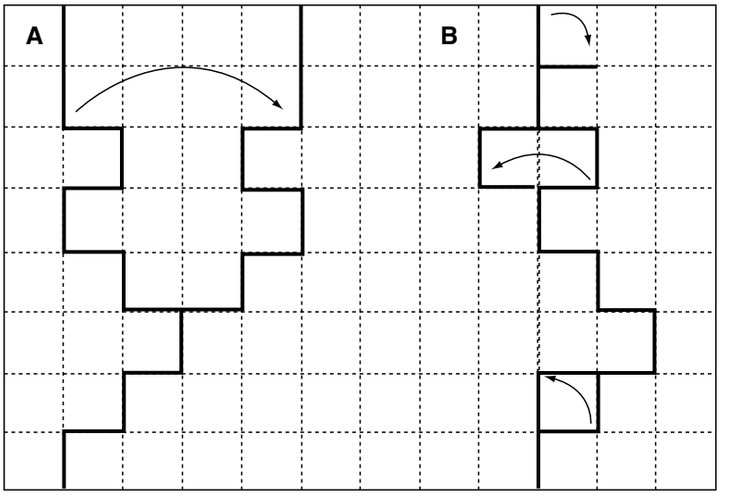

FIGURE 5.5. The idea of the pivot algorithm (A), and the local moves algorithm (B). The black contours indicate the initial structures, the lighter bonds show the accepted modifications. The local moves include (from top to the bottom of B): random chain end modification, a crankshaft move and a corner move.

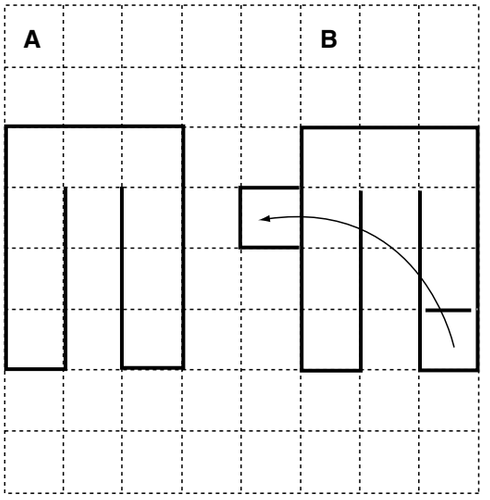

FIGURE 5.6. A trapped conformation for the algorithm with only local moves for a chain on the simple square lattice (A). A longer distance move that guarantees the ergodicity of the algorithm, where a U shaped fragment at one part of the chain is cut-off and attached somewhere else (B).

problems) of polymer dynamics is the difficulty of controlling the effects of the lattice anisotropy on the observed motion. Obviously, simple models of polymer conformations and dynamics, very similar to those described above could be design in the continuous space. Such models could be sampled using MD, MC, or via various hybrid sampling techniques based on a combination of genetic algorithms (GA) and molecular mechanics (usually MC dynamics). The results from simplified lattice and off-lattice models are essentially equivalent. For instance, the average chain dimensions of the real chain models scale as $\langle S^2 \rangle \sim n^{\gamma}$. Interestingly, the value of the universal constant for the 3-dimensional chains is close (but not identical) to the value resulting from the mean-field analytical theory of Flory. More qualitative differences are observed between the results of the "real" chain simulation of the polymer dynamics and the ideal chain theory of Rouse [37].

5.9.3 Simulations of Polymer Chain Collapse

Polymer chains in solution can undergo a collapse transition from an expanded random coil state to a dense globular state. The transition could be induced by decrease of temperature or by adding a "poor" solvent to the solution [41]. This process is difficult to describe analytically, but could be studied in details via computer simulations. Let us again consider a very simple lattice model. Representation of protein conformational state could be done using any kind of simple lattice. In such context it is easy to design a very simple potential mimicking the balance between the volume of the chain segments and their mutual attractions in the solution. The simplest form of such potential is given below:

$$E_{ij} = \begin{cases} \infty, for\ r_{ij} < 1 \\ \varepsilon, for\ r_{ij} = 1 \\ 0, for\ r_{ij} > 1. \end{cases} \quad (5.94)$$

In the formula above r_{ij} is the distance between two beads of the chain, 1 is the lattice spacing, and ε is a negative constant. With $\varepsilon = 0$ the model reduces to the model of a "real" chain in a good solvent, where mutual attractions of the chain segments could be ignored. Energy of the entire chain is a sum of the binary contributions ΣE_{ij}.

With decreasing temperature (or with increasing strength of the long-range interactions ε) the mean dimensions of the chain decrease (the solid curve in Fig. 5.7). The curves become steeper with increasing chain length; nevertheless the collapse transition remains continuous. The dashed horizontal line corresponds to the dimensions of an ideal chain of the same local geometry. The vertical dashed line denotes the collapse transition temperature. Slightly higher than ideal dimensions of the real chain at the transition midpoint are due to a bit higher prefactor – the scaling of the mean dimension with the chain length is at this point the same as for an ideal chain i.e., $\langle S^2 \rangle \sim n$. At very low temperatures, the globular state is a dense droplet with $\langle S^2 \rangle \sim n^{2/3}$. Obviously, at very high temperatures the chain behaves as the thermal "real" chain discussed in the previous section, i.e., $\langle S^2 \rangle \sim n^{\gamma}$.

Very interesting are the models where on top of the long range interactions a local stiffness of the model chain is superimposed. Let us assume that we are dealing now with a simple chain restricted to the diamond lattice (although any other lattice or off-lattice model can include the short-range interactions that simulate the polymer limited flexibility). Then let us assume that the *trans* conformation is favored energetically in respect to the two *gauche* conformations. At some critical ratio of the potential energy

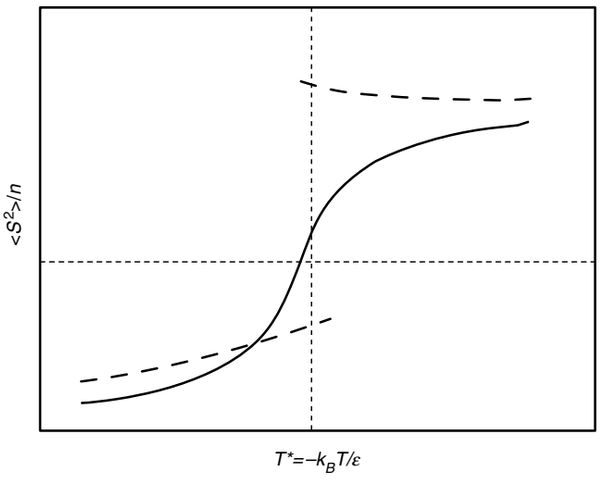

FIGURE 5.7. Collapse transition of a flexible polymer chain (solid line) and a semiflexible chain (dashed line) of a limited length (see the text for an explanation).

of these two types of local geometries the behavior of a chain of a limited length changes dramatically. In the range of high temperatures with decreasing temperature the chain dimensions increase due to increasing effect of the stiffness. Relatively long expanded segments could be seen at this range. At a critical temperature, these ''rods'' of fluctuating length coalesce due to a huge decrease of the potential energy of the long-range interactions for a small entropic expense. The transition is abrupt, highly cooperative (the average length of the expanded sequences jumps up at the transition), and has all features of the first-order phase transition, including easily detected metastable region, an ''almost'' singularity of the heat capacity and an extremely low population of the intermediate states. At the transition midpoint the simulated molecules adopt essentially only two types of conformations; swollen random coils with a short sequences of expanded states and a densely packed, highly ordered globular state, with much longer sequences of the expanded local conformations. This behavior of the semiflexible model has a number of essential properties of globular proteins. First, the collapse transition is pseudo first-order (all-or-none in the language of protein biophysics). Second, it is cooperative and the collapse induces a sudden increase of the length of the regular expanded fragments, very much as the formation of secondary structure during the protein folding transition. Third, the collapsed structure is highly ordered with relatively well defined (however not unique) number of ''secondary structure'' expanded elements. Note, that these striking similarities are observed in the homopolymer model where all polymer units are the same. This leads to the conclusion that one of the most important general aspects of protein folding is a competition between the long-range and the short-range (stiffness) interactions. In this picture, differentiation of the interactions along the polypeptide chains (sequence of amino acids) plays a ''fine-tuning'' role, selecting the structural detail of the globular state. This analogy to protein folding extends even further. As the length of the semiflexible chain increases the ordering of the globular state becomes modular – domains are formed upon the collapse. Each domain can form at slightly different temperature, within the range of the metastable states shown in Fig. 5.7. When the number of domains becomes large the collapse transition becomes continuous, as it should be for any infinitely long flexible (or semiflexible) polymer chain. Such detailed insight into the collapse transition of semiflexible polymers could be gain only from computer simulations, although a very approximate theories for a single globule collapse of semiflexible polymers were published in past.

A single polymer simulations could address also the issues of chain topology, including the effect of polymer branching and macrocycles on the thermodynamics of the collapse transition and the dynamics in a diluted media. This can be addressed on various levels of details, from a large scale conformational sampling within a framework of reduced models to a detailed molecular mechanics study of local conformational transitions. For instance, a very interesting simulation of DNA collapse has been recently performed using the bead and string model with a short range bending potential and the Brownian Dynamics as a sampling technique. These simulations led to a very plausible and nontrivial picture of the DNA collapse pathway. It is also possible to employ a multiscale sampling, where the large scale relaxations are modeled on a low resolution level and the details are studied with the all-atom representation.

Finally, it is worth to mention a very broad class of approaches to a specific problem of polymer collapse transition, the protein folding transition. This field attracts a lot of researches due to its importance for molecular biology, and biotechnology, genetics, and molecular medicine (including new drugs design in particular). In the case of the protein folding problem, the details of physics and the pathway description of the collapse transition are (at least by now) of a lesser importance. The mean goal is to predict the unique structure of protein globular state. The task is nontrivial, since the copolymers of interest are composed of twenty different mers (amino acids) and the sequence of these mers dictates a vast variety of three-dimensional globular structures, with a very specific local conformations and their well defined mutual packing in the globule. Two types of algorithms are now the most successful. The first one uses a large set of ''prefabricated'' protein fragments, extracted from a collection of known three-dimensional structures, and the sampling scheme are based on an iterative shuffling of these fragments within the simulated chain. Another approach is more in spirit of the classic polymer algorithms. It employs a local move schemes, however with a complex representation of the polypeptide conformational space and elaborated set of mean field potentials, derived either from the physical properties of the small molecules or from statistical analysis of the structural regularities seen in known structures of globular proteins. An amazing progress was achieved in this field during the last few years. The second approach is probably somewhat more general; it opens a possibility of a qualitative study of protein folding pathways and molecular mechanisms, not only the predictions of the globular structure. The predictive power of the both type of approaches are similar. Nevertheless, the second one seems to be a bit more open for a wider range of applications. These applications include the bootstrapped (resolution- and time-vise multiscale) implementations of the polypeptide representation and dynamics. Coupling of the various levels of resolution enables for a quite detailed study of protein dynamics and thermodynamics. The simulation techniques and models developed specifically for proteins are easily adaptable for more general applications in polymer computational physics. [43]

5.9.4 Simulations of Dense Polymeric Systems

Dense polymeric systems include polymer solutions, polymer networks, polymer melts, polymer liquid crystals

and solids, and many more. There is a vast body of literature on each of these subjects [42]. The modeling approaches are also of great variety, from a simple reduced models (lattice and continuous) to the detailed molecular mechanics and even a quantum mechanics. It is beyond scope of this chapter to go through the detail of various applications. Let us just outline some of problems that could be addressed in computer simulations, increasing our understanding of complex systems and providing important stimuli for theoretical studies and practical applications in material science and biotechnology.

Typical dense polymer solutions and melts are globally disordered; however the level of local ordering could be relatively high. This is a very complex phenomenon that involves long-range correlations that are the results of specific local interactions. A general insight could be gain from the low resolution models that allow for study of the large scale conformational rearrangements; although specific details could be very sensitive to the atomic structure and require extensive molecular mechanic study of carefully selected starting conformations. The same could be said about the phase transitions in bulk polymers.

The rate polymer diffusion in polymer media spans orders of magnitude. The mechanism of the process is unclear. It is very difficult to provide even a qualitative mechanistic picture how a long chain can move throughout a complex network of entanglements superimposed by the other macromolecules. The reptation theory of DeGennes [13] is probably only qualitatively true and only for very specific conditions. Simulations could be extremely helpful in at lest qualitative understanding of this process.

Another challenging (however not really macromolecular) polymeric system are biological membranes. It is known from various experiments that the spectrum of relaxation processes in membranes is extremely wide; from local cooperative motion of phospholipide chain and occasional jumping of molecules from one side of a membrane to the other one to a global flexing of the membrane and formation of vesicles. Simulations are done on various levels of generalization. There are mesoscopic model which treat the membrane as a kind of elastic network, but also a very detailed all-atom study of membrane structure and local dynamics. Bootstrapped, multiscale simulations could be a very promising way to attack this problem.

REFERENCES

1. W.L. Mattice and U.W. Suter, *Conformational Theory of Chain Molecules*, Wiley, New York, 1994.
2. M.F. Schulz and F.S. Bates, this volume, Chap. 32
3. H. Yamakawa, *Modern Theory of Polymer Solutions*, Harper & Row, New York, 1971.
4. A.Y. Grosberg and A.R. Khokhlov, *Statistical Physics of Macromolecules*, AIP, New York, 1994.
5. M. Warner and E.M. Terentjev, *Liquid Crystal Elastomers*, Oxford University Press, Oxford, 2003.
6. J.E. Mark and B. Erman, *Rubberlike Elasticity. A Molecular Primer*, Wiley, New York, 1988.
7. B. Erman and J.E. Mark, *Structures and Properties of Rubberlike Networks*, Oxford University Press, Oxford, 1997.
8. A. Kloczkowski, M.A. Sharaf and J.E. Mark, *Chem. Eng. Sci.* **49**, 2889 (1994).
9. M.A. Sharaf and J.E. Mark, *Polymer*, **45**, 3943 (2004).
10. W. Zhao and J.E. Mark, this volume, Chap. IIB.
11. J.D. Honeycutt, this volume, Chap. IIID.
12. K.F. Fried, *Renormalization Group Theory of Macromolecules*, Wiley, New York, 1987.
13. P.G. DeGennes, *Scaling Concepts in Polymer Physics*, Cornell University Press, New York, 1979.
14. J. des Cloizeaux and C. Jannink, *Polymers in Solutions: Their Modeling and Structure*, Clarendon, Oxford, 1990.
15. W.C. Forsman, Ed., *Polymers in Solution*, Plenum, New York, 1986.
16. K. Binder, Ed., *Monte Carlo Methods in Statistical Physics*, Springer-Verlag, Berlin Heidelberg New York, 1986.
17. K. Binder, *Monte Carlo and Molecular Dynamics Simulations in Polymer Sciences*, Oxford University Press, Oxford, 1995.
18. A. Baumgaertner, Simulation of polymer motion, *Ann. Rev. Phys. Chem.* **35**, 419 (1984).
19. Kolinski and J. Skolnick, *Lattice Models of Protein Folding, Dynamics and Thermodynamics*. R.G. Landes, Austin, TX, 1996.
20. M. Kotelyanskii and D.N. Therodorou, Ed., *Simulation Methods for Polymers*, Marcel Dekker, New York, 2004.
21. P.J. Flory,*Statistical Mechanics of Chain Molecules*, Interscience, New York, 1969.
22. J.D. Honeycutt, this volume, Chap. XX.
23. P.J. Flory, *Proc. Roy. Soc. London, Ser. A* **351**, 351 (1974).
24. H.M. James and E. Guth, *J. Chem. Phys.* **15**, 669 (1947).
25. A. Kloczkowski, J.E. Mark and B. Erman, *Comput. Polym. Sci.* **2**, 8 (1992).
26. P.J. Flory, *J. Chem. Phys.* **66**, 5720 (1977).
27. B. Erman and L. Monnerie, *Macromolecules*, **22**, 3342 (1989), **25**, 4456 (1992).
28. A. Kloczkowski, J.E. Mark and B. Erman, *Macromolecules*, **28**, 5089 (1995).
29. R.T. Deam and S.F. Edwards, *Phil. Trans. R. Soc, A,* **280**, 317 (1976).
30. R.C. Ball, M. Doi and S.F. Edwards, *Polymer*, **22**, 1010 (1981).
31. T. Vilgis and B. Erman, *Macromolecules*, **26**, 6657 (1993).
32. D.S. Pearson, *Macromolecules*, **10**, 696 (1977).
33. P. Debye, *J. Phys. Colloid. Chem.* **51**, 18 (1947).
34. R.H. Boyd and P.J. Philips, *The Science of Polymer Molecules*, Cambridge, New York, 1993.
35. P.R. Schleyer, Ed. *Encyclopedia of Computational Chemistry*, Wiley, New York, 1998.
36. W.F. van Gunsteren and P.K. Weiner, *Computer Simulations of Biomolecular Systems. Theoretical and Experimental Applications.* Escom, Leiden, 1989.
37. P.E. Rouse, *J. Chem. Phys.* **21**, 1272 (1953).
38. M. Doi and S.F. Edwards, *The Theory of Polymer Dynamics*, Clarendon, Oxford, 1986.
39. P.H. Verdier and W.H. Stockmayer, *J. Chem. Phys.* **36**, 227 (1962).
40. M. Rosenbluth and N. Rosenbluth, *J. Chem. Phys.* **23**, 356 (1955).
41. A. Montesi, M. Pasquali and M.C. MacKintosh, *Phys. Rev. E* **69**, 021916 (2004).
42. J.E. Mark, K. Ngai, W. Graessley, L. Mandelkern, E. Samulski, J. Koenig and G. Wignall, *Physical Properties of Polymers,* Cambridge University Press, Cambridge 2004.
43. A. Kolinski, Acta Biochim. Polonica **51**, 349 (2004).